Gelation Kinetics of Gelatin: A Master Curve and Network Modeling

Valéry Normand,*,† Stéphane Muller,† Jean-Claude Ravey,† and Alan Parker‡

Laboratoire de Physico-Chimie des Colloides, LESOC, Université Henri Poincaré, BP 239, 54506 Vandoeuvre, France; and Food Ingredient Division, Research Center, SKW Biosystems, 50500 Carentan, France

Received June 14, 1999; Revised Manuscript Received September 8, 1999

ABSTRACT: The gelation kinetics of gelatin has been exhaustively studied using oscillatory rheometry for six molecular weight distributions, three concentrations, and four temperatures. Measurements lasted up to $3^1/_2$ months, much longer than previous studies. Remarkably, all of the data can be superimposed on a single master curve using suitable shift factors. The existence of a master curve shows that, over the broad range of variables studied, the gelation processes are identical; altering the variables just changes the scaling factors for elasticity and time. Empirically, it is found that neither high nor low molecular weight chains contribute to the elasticity. A statistical network model has been developed, based on Flory's phantom network formalism. It gives reasonable fits to the experimental gel times and is compatible with the observed dependence of elasticity on molecular weight distribution. A second order reaction kinetics model has also been developed which satisfactorily models the early stages of gelation.

Introduction

Gelatin is by far the most widely studied functional biopolymer, initially due to its use in glue and then due to its use in the photographic and food industries, among others. It is prepared by degradation of collagen. As early as 1964, Veis wrote a 400 page monograph[1] on the subject, which can still be read fruitfully. Because of its industrial importance, the gelation of gelatin has been widely described in the literature from the sol−gel transition to the fully formed gel.[2,3,4] It has also served as an archetype for fundamental studies of physical gels for decades. Gelatin in water at concentrations up to 300 g/L forms low viscosity solutions at temperatures above 40 °C. On cooling, these solutions start to form clear, rubbery, thermoreversible gels at temperatures close to room temperature. The cross-links are due to the formation of segments of intermolecular triple helix. These have the same structure as collagen.

The approximate c^2 dependence of the elasticity of gelatin was first established as early as 1904, according to Veis,[1] and has been confirmed in numerous studies since. Coopes[5] first postulated a model to explain how the known triple helix form of the junction zones is compatible with a c^2 concentration dependence. He suggested that the triple helical cross-links are made up of only two chains, but one turns back on itself to contribute two of the three component strands. This idea was later confirmed by Benguigui et al.[6] using enzymatic degradation.

Ferry and Eldridge[7] studied the effect of the average molecular weight on the elastic modulus of gelatin gels. They found that the modulus was proportional to the square of the weight-average molecular weight. However the samples were highly degraded with average weights in the range from 30 000 to 70 000. Saunders and Ward[8,9] studied the modulus of fractionated gelatin of higher molecular weight and found that the modulus plateaued for average molecular weights higher than those studied by Ferry and Eldridge. At the highest molecular weights, the rigidity even decreased slightly.

A factor, which has been neglected in these studies, is the molecular weight distribution. In fact, the majority of studies have used a single sample of gelatin, often of unknown molecular weight. Therefore, it is impossible to compare them and decide whether their conclusions are general or not.

To improve this situation, the gelation kinetics of six different samples of commercial gelatin have been compared. They were obtained from the same batch of raw material, by extraction under increasing severe conditions, so that they were quite similar chemically but had different molecular weight distributions. A range of concentrations and cure temperatures was used for each sample, resulting in a set of 72 different gelation kinetics. The results are first analyzed using a semiempirical master curve approach, following its successful application by Meunier et al.[10] to the gelation kinetics of κ-carrageenan. Then the data are interpreted using Pearson and Graessley's statistical network model,[11] which is based on the Flory phantom network formalism.[12] Finally, the early stages of the gelation kinetics are modeled, using a simple second-order reaction scheme.

Materials and Methods

Commercially extracted gelatin samples were provided by SKW Biosystems (Paris, France). They were produced by alkaline degradation of bovine bone at high temperatures for long times (weeks). The extract number (x) increases with the severity of the extraction. Low numbers correspond to high gelling power. The manufacturer determined the molecular weight distributions, using a high performance size exclusion chromatograph fitted with a refractive index detector. The columns were calibrated using gelatin samples with known absolute molecular weight distributions. Figure 1 shows a typical molecular weight distribution, that of sample E1. The distribution can be divided into three broad molecular weight classes. The original molecule of collagen (single chain) is called a α chain and is the simplest result of the denaturation. However, the denaturation process also leads to secondary products due to random scission of single collagen molecules. In the gelatin industry these hydrolyzed α chains are called "small units". Alkaline hydrolysis is sometimes incomplete, leaving covalent bonds between molecules. Two or three α

† Université Henri Poincaré.
‡ SKW Biosystems.

10.1021/ma9909455 CCC: $19.00
Published on Web 01/18/2000

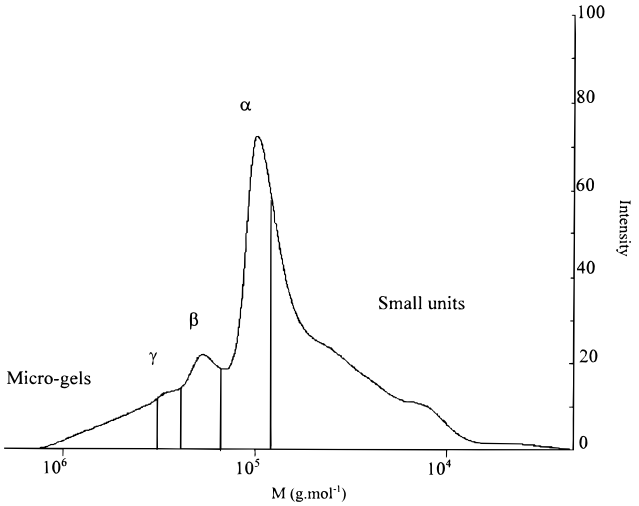

Figure 1. Molecular weight distribution of sample E1.

Table 1. Molecular Weight Distributions by Molecular Weight Class for the Six Gelatin Samples

	E1	E2	E3	E4	E5	E6
$M > 10^6$	0.32	2.04	4.05	8.05	2.77	0.39
$10^6 > M > 5.4 \times 10^5$	3.86	10.31	12.92	13.83	7.71	2.48
tetra and penta	5.82	9.69	11.12	9.68	6.61	3.51
microgels	10.00	22.04	28.09	31.56	17.09	6.38
γ chains	7.70	9.94	10.00	8.33	6.49	4.59
β chains	17.78	17.78	17.43	14.76	13.74	12.31
α chains	28.75	20.65	16.69	14.08	13.76	13.28
$\Sigma(\alpha + \beta + \gamma)$	54.23	48.37	44.12	37.17	33.99	30.18
$10^5 > M > 5 \times 10^4$	17.20	13.28	11.44	11.15	13.48	14.78
$5 \times 10^4 > M > 3 \times 10^4$	7.00	5.91	5.63	6.27	9.52	11.67
$3 \times 10^4 > M > 2 \times 10^4$	4.38	3.77	3.72	4.51	7.81	10.27
$2 \times 10^4 > M$	7.19	6.63	7.00	9.34	18.11	26.72
small units	35.77	29.59	27.79	31.27	48.92	64.44
total	100.00	100.00	100.00	100.00	100.00	100.00

chains linked together are called respectively β or γ chains. When more than three α chains are covalently linked, the macromolecules are called "microgels", in the industry. Table 1 summarizes the results for all six extracts in terms of these different molecular weight classes. The proportion of each molecular weight class in a particular batch of gelatin depends first on the raw material and second on the conditions, temperature and duration of the denaturation. For samples E1−E4, the temperature and pH of extraction were the same. Only the denaturation time increased with the extract number. However, for samples E5 and E6, the pH and the temperature of the alkaline solution were increased to dissolve the last remaining collagen. This difference in the production process is clearly reflected in the molecular weight distributions (see Table 1). As the extract number increases, the fraction of α, β, and γ chains decreases, the fraction of small units increases and the fraction of microgel decreases.

All gelatin concentrations are quoted in percent weight for weight. Solution preparation was in three stages. First the gelatin grains were left to swell in deionized, twice distilled, water under slow stirring, at room temperature for 60 min. A homogeneous solution was formed by heating the dispersion at 55 °C for 35 min under slow agitation using a magnetic stirrer. Finally, the sample was held at 40 °C for 30 min prior to measurement. A 500 ppm sample of sodium azide (NaN_3) was added to prevent bacterial degradation, and a thin film of dodecane was placed on top of the solution to prevent evaporation.

Gelation kinetics were followed by small deformation oscillatory measurements using a Carrimed CSL 500 stress-controlled rheometer. The specially designed measurement cell has been described previously.[13] It has a double concentric cylinder geometry, but only the outer gap was filled with sample. It has two major advantages: (i) it can be repeatedly removed from the rheometer and replaced without disturbing the sample, so that gelation can be followed for long periods without blocking the rheometer; (ii) the sample forms a three-dimensional ring trapped between layers of inert, nonvolatile liquids (dodecane above and perfluorodecalin below). This arrangement eliminates end effects, evaporation losses, and two-dimensional gel network formation. Once filled, the measurement system was placed in a temperature-controlled holder, and the sample was cooled from 40 °C to the measurement temperature, in 2 min, independent of the measurement temperature. Measurements were made at a frequency of 1 Hz and at constant strain amplitude of 2%, which was in the range of linear viscoelasticity. Measurements were not made during the first 3 min at the cure temperature, as it was found that this could cause irreversible damage to the gels, especially when weak gels were measured.

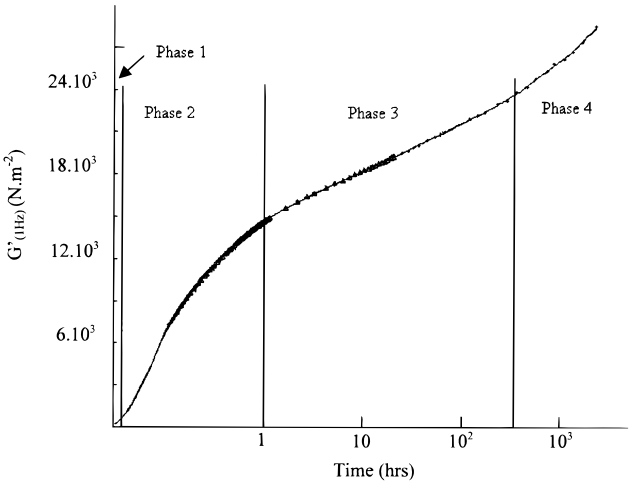

Figure 2. The four phases of the gelation kinetics (sample E1 at 10% and 5 °C).

Results

The gelation kinetics of all six samples were measured at three different concentrations (3%, 6.66%, and 10%) and four different temperature (5, 10, 15, and 20 °C) for at least 20 h. The elasticity of certain gels was followed for up to $3^1/_2$ months, much longer than previous studies. All of the cure curves had the same shape. Figure 2 shows a typical example. The gelation kinetics can be divided into four phases.

(1) The loss modulus, G'', (not shown here) is higher than the elastic modulus, G', and, to a first approximation, the gelatin solution is still liquid. The frequency independent, gel time is defined as occurring when $G'(\omega)$ is parallel to $G''(\omega)$ over a large frequency range, with $G''(\omega) > G'(\omega)$.[14] However, it was not possible to follow the kinetics of gelation at frequencies significantly lower than 1 Hz in the early stages of gelation, because the measurement time must be significantly shorter than the rate of change of the viscoelastic properties.[15] The measurement frequency (1 Hz) was chosen as the best compromise between the low frequency needed to measure the equilibrium modulus and the high frequency needed to track the gelation kinetics with good precision, as discussed by Mours and Winter.[15] Under these conditions, the crossover between G' and G'' at 1 Hz has been retained as a convenient definition of the gel point, even though Michon et al.[16] have shown that it is not exact for gelatin gels. The rapid change of the elasticity

close to the gel point makes the error in the gel time induced by this approximation small (less than 5%).

(2) A gel forms, and both G' and G'' increase rapidly, which indicates fast formation of junction zones and strong reinforcement of the gel structure. It has been suggested[17] that the three-dimensional network is built at this stage and that the reinforcement is due to the formation of new cross-links. This idea is corroborated by an important observation that seems not to have been made previously: if a gel is cut after only 30 min of cure, it will subsequently heal. In almost all cases, this second phase ends after roughly 1 h of gelation, independent of the molecular weight distribution, concentration, or temperature. The only exceptions were a few of the weakest gels, which had long gel times. These were made from samples E5 and E6 at the lowest concentration (3%) and highest temperatures (15 and 20 °C).

(3) From 1 h to 100 h, G' increases more slowly: it is linear with the logarithm of time. This phase lasts several hundred hours, the exact time depending on the molecular weight distribution, the temperature, and the concentration. This second elasticity increase is assumed to be mainly due to the extension of existing cross-links rather than the formation of new ones.[18] This explanation is corroborated by (i) the fact that a gel cut after more than 1 h of cure does not heal and (ii) by the constant value of G'' during this phase (results not shown). Djabourov[19] has extensively described these last two phases using rheological and polarimetric measurements in parallel.

(4) Figure 2 shows that at very long cure times another phase occurs in which the slope of G' vs the logarithm of time is larger than in the third phase. We have two hypotheses for this behavior: the first is that it might be an experimental artifact due a slight increase in concentration, caused by slow diffusion of water through the dodecane layer. The second is that the increase in slope could be due to a genuine structural change in the gel. This possibility is discussed below in the section on network modeling.

The Effect of Temperature. The extreme sensitivity of gelatin gels to temperature is well-known. Figure 3a shows that, at constant concentration and molecular weight distribution, as the cure temperature increases, the gel strength decreases, but the shape of the cure curve remains unchanged. The lower moduli at higher temperatures are probably a consequence of a lower concentration of junction zones. These junction zones begin to age after 1 h and the slope of G' vs the logarithm of time decreases with increasing cure temperature.[20] Figure 3b shows the elastic modulus of sample E1 at a concentration of 6.66% for different cure times (12 min, 1 h, and 20 h) and different cure temperatures. G' is a linear function of the cure temperature. For each cure time, the linear fit can be extrapolated to give a limiting temperature at which G' is zero. We interpret these limiting temperatures as the cure temperatures for this system which lead to gelation times of 12 min, 1 h, or 20 h. We found (results not shown) that gelation (i.e., $G' = G''$) always occurred when G' was $\approx$ 1 Pa, so this is a good approximation.

Explaining the effect of temperature on gelatin gelation is difficult, as there is a complex interplay between kinetic and thermodynamic factors. The main conclusion, however, is that, for any given cure time, the elastic modulus decreases linearly with the temperature.

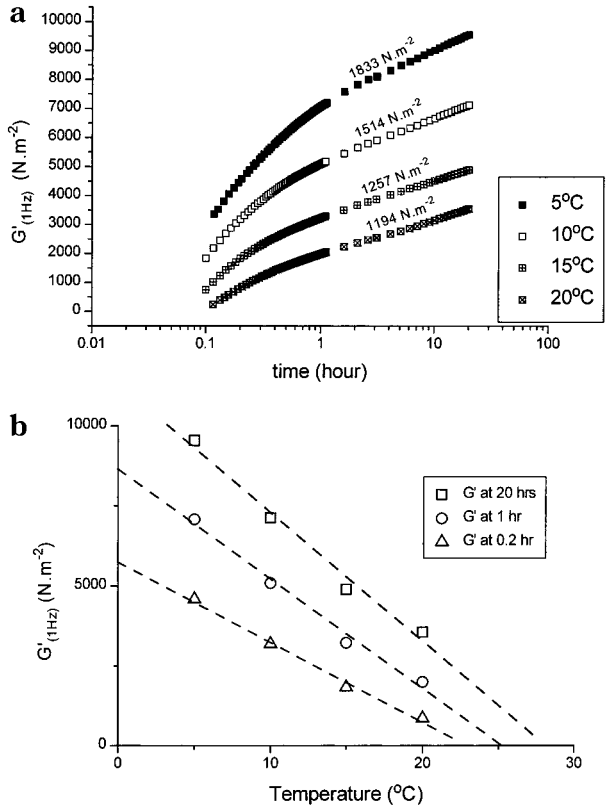

Figure 3. (a) Gelation kinetics of sample E1 at 6.66% for four different temperatures. Figures indicate slopes during the third phase. (b) Evolution of the modulus after different measurement times as a function of the temperature for sample E1 at a concentration of 6.66%.

The Effect of Concentration. The effect of concentration on the rheological properties of gelatin gels has already been widely investigated. It has been treated theoretically by modeling the dependence of the elastic modulus as a function of the concentration, using the cascade model.[3] A well-known result, already reported by several authors, is that G' is proportional to the square of the concentration,[3,21] over the concentration range used here. However, when the concentration increases much above 10%, a dependence of less than a power of 2 is suggested by the cascade approach, and at concentrations below 3% the exponent increases to values much greater than 2.

Figure 4 shows the logarithm of G' plotted against the logarithm of concentration for the same cure times as in Figure 3. A relationship in c^2 was found for cure times in the third phase of gelation (see Figure 2), but a higher exponent is suggested for cure times in the second phase (we found 2.3 when the aging time was 12 min). However, this last result is somewhat uncertain as, at low concentrations, the gel time changes significantly under the experimental conditions chosen. While the effect of differences in gel time can be neglected for high concentrations, they cause large differences in cure times at low concentrations, as our reference time t_0 is the time at which the cooling step starts. If the data corresponding to 3% concentration are eliminated, the slope for concentrations 6.66% and 10% is 2.0 even after only 12 min of cure.

The Effect of the Molecular Weight Distribution. Figure 5 shows the gelation kinetics for all six samples

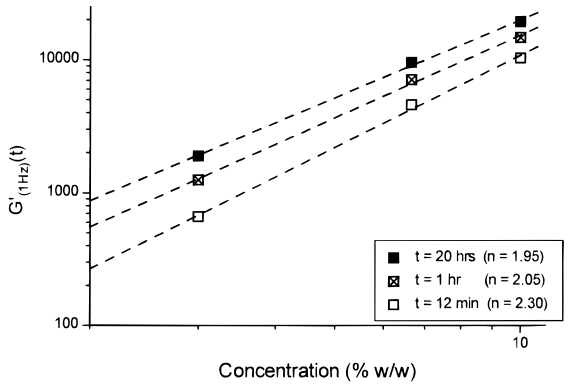

Figure 4. Elastic modulus as a function of concentration for different cure times, evolution of the exponent with aging time. Sample E1 at 5 °C.

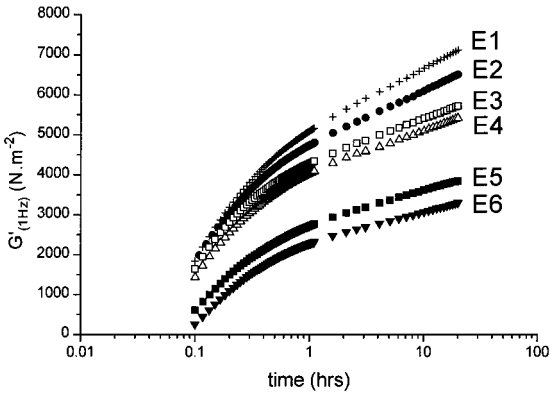

Figure 5. Comparison of the gelation kinetics for different samples, at 6.66% concentration and 10 °C.

at a concentration of 6.66% and a temperature of 10 °C. The results clearly fall into two groups: the first group includes samples E1−E4 and the second includes samples E5 and E6. This difference is certainly due to the more severe conditions used to extract the last two samples, which reduces their gelling power, as discussed under Materials and Methods.

We searched for a simple relationship between the elasticity and the molecular weight distribution using regression analysis and heuristics. Good results were found by making the extremely simple assumption that the α, β, and γ chains contribute equally to the elasticity, while the smaller and larger molecules contribute nothing. Although a negligible contribution of the low molecular weight fractions seems reasonable intuitively, it is surprising that the large molecular weight fractions do not contribute. Veis (p 406 of ref 1) explains this by suggesting that the helical junction zones in which these molecules participate are more or less exclusively intramolecular. Figure 6 shows the power law relationship between the elastic modulus, and the $\alpha + \beta + \gamma$ chain content at constant temperature and concentration. The figures on the graph indicate the power law exponents for the different cure times. Sample E4 does not follow the same trend as the five other extracts. We speculate that this might be due to an error in the measurement in the molecular weight distribution. Nevertheless, Figure 6 shows that, for all six samples, the effects of the molecular weight distribution can be quite well explained in terms of an *effective* concentration, which is given by the total gelatin concentration multiplied by the fraction of chains in α, β or γ form. The power law exponent relating the modulus to the effective concentration varies with time, from 2.6 at small aging times to 2.0 at long aging times. This trend has already been shown in Figure 4. This result implies that the formation of the gel network is more concentration dependent at the early stages of the gelation than at later stages.

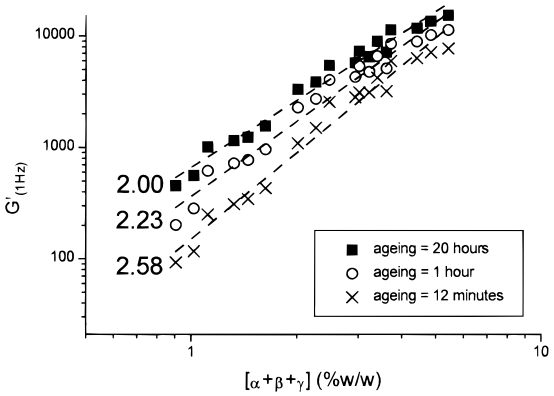

Figure 6. G' as a function of the effective concentration for three different aging times at 10 °C. Slopes are indicated on the graph.

A Master Curve for the Gelation Kinetics. Meunier et al. have recently shown[10] that the gelation kinetics of κ-carrageenan, measured at different temperatures and concentrations, can be superposed to form a unique master curve by suitable shifts along the elasticity and time axes. κ-Carrageenan is a helix-forming polysaccharide, which aggregates on cooling to form thermoreversible gels. We attempted the same exercise, but also included the effects of the molecular weight distribution, by using the effective concentration, instead of the total concentration. The reference curve was the data from sample E1 under the conditions of the industry standard (Bloom) gel strength test: 6.66% concentration and 10 °C. Figure 7a shows that the 72 different gelation kinetics can be superposed to form an extremely satisfying master curve. Only the result for sample E6 cured at the lowest concentration and highest temperature diverged significantly, probably due to its abnormally long gelation time, as discussed above.

It was found empirically that the vertical and the horizontal shift factors show an approximate power law relationship with the effective concentration and the temperature. These have been summarized in eqs 1 and 2, where c_{eff_0} is the effective concentration of sample E1 at 6.66% and T_0 is 10 °C.

$$G' = \left(\left(\frac{c_{\mathrm{eff}}}{c_{\mathrm{eff}_0}}\right)^{2.03\pm0.2}\left(\frac{T}{T_0}\right)^{-1.01+0.06}\right)G'_0 = e^{a_{G'}}\,G'_0 \quad (1)$$

$$t = \left(\left(\frac{c_{\mathrm{eff}}}{c_{\mathrm{eff}_0}}\right)^{-0.86\pm0.18}\left(\frac{T}{T_0}\right)^{0.75\pm0.06}\right)t_0 = e^{a_t}t_0 \quad (2)$$

The temperatures T and T_0 are expressed in degrees Celsius.

The concentration exponents were estimated by a fit to 18 experimental results: six extracts at three concentrations and 10 °C. The temperature exponents were estimated by a fit to four experimental results: extract E1 at 6.66% and four different temperatures.

Figure 7b shows the comparison between calculated and experimental shift factors for the whole set of results. Reasonable agreement is obtained for most of the samples with standard deviations being respectively 4% and 11% for $a_{G'}$ and a_t. However, eqs 1 and 2

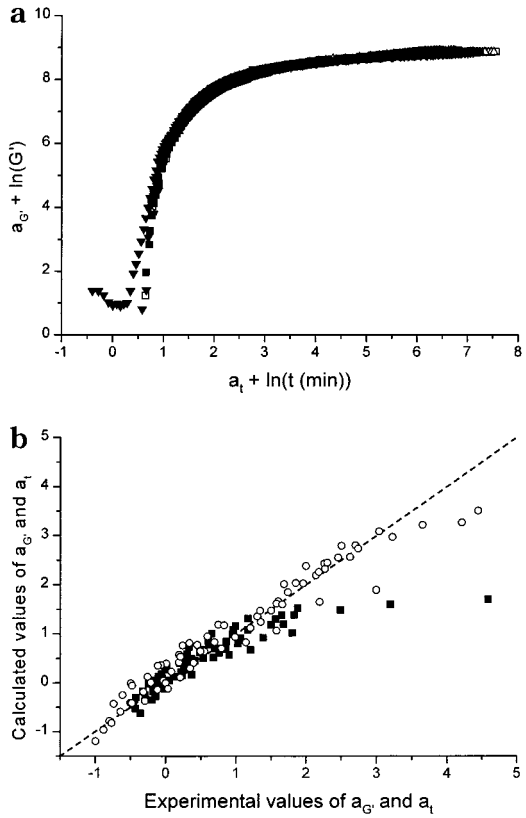

Figure 7. (a) Master curve for the gelation kinetics of gelatin. Reference: sample E1 at 6.66% and 10 °C. (b) Comparison of the experimental shift factors and shift factors calculated via eqs 1 and 2. Key: Solid squares, a_t;, open circles, $a_{G'}$; dotted line, slope 1.

systematically underpredict the experimental values when the shift factors are large ($a_t > 2$ and $a_{G'} > 3$). These correspond to the results for samples E5 and E6 cured at low concentration and high temperature, probably because of their long gelation times. Clearly, an improved fit could be obtained by adding extra terms to eqs 1 and 2.

Note that the fit of the experimental shift factors to eqs 1 and 2 is not a measure of the correctness of the master curve approach. However, it does allow the shifts for the full set of results to be compared and shows that the deviations seen in Figure 7b are self-consistent. This in turn demonstrates the self-consistency of the set of experimental results.

Once again, the elasticity is best fit by a c^2 dependence. However, in this case, the fit is to a master curve, so it is independent of time, temperature, and molecular weight distribution, contrary to all previous studies. On the other hand, the linear temperature dependence of the elastic modulus, which has already been presented in Figure 3b, is a new result. As shown by eq 2, the time follows approximately a c^{-1} and T^1 dependence. However, both Oakenfull[22] and Ross-Murphy[23] observed a larger dependence of the gel time (time when $G'_\omega \propto G''_\omega \propto \omega^\Delta$) on concentration, respectively $t_g \propto c^{-3}$ to $t_g \propto c^{-2}$. In light of these results, it seemed natural to attempt to form a master curve for the loss modulus, but in fact this was a complete failure. This result suggests that the loss modulus cannot be shifted in time using the same shift factors (a_t) as the elastic modulus. It seems that the loss modulus is an intrinsic property of the network, related to the molecular weight distribution of the gelatin samples in another way than the elastic

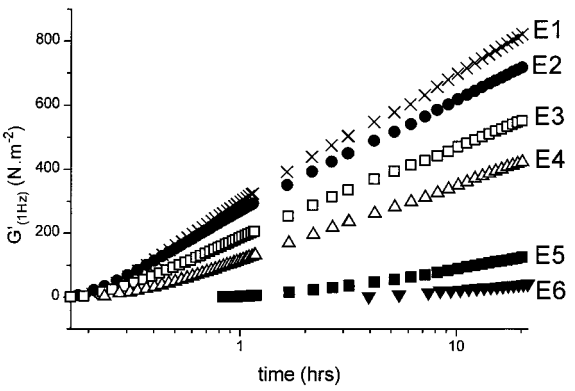

Figure 8. Gelation kinetics for the six samples at 3% and 20 °C.

modulus, and the gel time depends on its evolution with time as the network forms.

In principle, this model, together with a single elasticity measurement at one temperature and one concentration, can be used to calculate the whole gelation kinetics of a gelatin sample, from when it sets to several months later, at any concentration or temperature within the range studied here. In fact, a suitable measurement is made for all commercial samples of gelatin. They are invariably supplied with a "Bloom" value, which defines a sample's gelling power and is directly proportional to its elastic modulus at a concentration of 6.66% after 16 h at 10 °C.

Note that this master curve has only been verified here for one particular manufacturing process and one particular raw material: alkaline-treated bovine bones, which are the source of most photographic gelatin. Its validity would have to be checked for other processes and other raw materials, such as acid-treated pigskin, which is the main source of gelatin for the food industry.

Network Modeling. A network model is needed to understand the relationship between the elasticity of gelatin gels and the molecular weight distribution. The model used here for describing the growth of the network with time is that of Pearson and Graessley.[11] Their results are only presented and used here. Readers should refer to the original publication for the full expressions and their derivation. They made use of Flory's simplifying assumption that the cross-link volume is negligible (the so-called phantom network).[24] This assumption is best fulfilled when the concentration is low and the cure temperature is close to the critical gel temperature, so we have focused on the results obtained at 3% concentration, and 20 °C cure temperature, which are shown in Figure 8. The aim is to determine the number of fundamental circuits (ξ) in the network. This parameter is directly related to the gel elastic modulus by

$$G \approx \frac{\Phi \xi kT}{V_0} \tag{3}$$

Φ is a constant, assumed to be close to unity for gelatin gels, which depends on the connectivity of the network. k is the Boltzman constant. T is the absolute temperature, and V_0 is the volume of the network. This equation can be rewritten in molar terms as

$$\frac{\Phi \xi kT}{V_0} = \frac{\xi}{N} \frac{cRT}{\overline{M_n}} \tag{4}$$

N is the number of gelatin chains involved in the network, c the concentration of the chains involved in the network elasticity (in g L^{-1}), R the gas constant and $\overline{M}_n$ the number-average molecular weight of the chains which contribute to the network elasticity. Pearson and Graessley linked ξ to two structural parameters of the network: the number of elastically active junction zones (μ) and the number of elastically active network chains (EANCs) (ν). The definition of an EANC used here is the same as that of Scanlan[25] and Case:[26] a portion of gelatin molecule is active if it is connected at both ends to junction zones with at least three paths to the gel boundary. The relationship linking these three parameters is

$$\xi = \nu - \mu + 1 \tag{5}$$

Furthermore, ν and μ are related to α, the fraction of structural units participating directly in cross-links via eqs 6 and 7. (it is unfortunate that the symbol α is used here to signify both a molecular structure and the extent of reaction; however both are very well established. It is always clear which is intended.)

$$\nu = \frac{1}{2}\alpha r N P \tag{6}$$

where P is a statistical parameter representing twice the number of cross-linked units with two paths to the gel multiplied by the probability that they are cross-linked to units with at least one path to the gel, plus the number of cross-linked units with one path to the gel, multiplied by the probability that they are cross-linked to units with at least two paths to the gel. The factor $^1/_2$ corrects for the double counting of all strands.

$$\mu = \alpha r N Q \tag{7}$$

where Q is the total number of junctions minus those with only zero, one, or two paths to the gel.[11]

Djabourov[27] and Durand[28] showed experimentally that there is a critical degree of helix conversion at the gel point. This observation allows the introduction of a critical value of α for which a gel can exist. This critical fraction of cross-linked units at the gel point, α_c, is given by

$$\alpha_c N[r - 1] = \frac{N}{(f_w/2 - 1)} \tag{8}$$

where r is the number of structural units per chain and f_w is the weight-average number of chains leading away from a randomly selected junction zone. By definition, the critical concentration of cross-links at the gel point is given by $\alpha_c N[r - 1]$. According to eq 8, each chain has one cross-link on average at the gel point, which is the criterion for the existence of the infinite gel network, and the ratio α/α_c is the reduced cross-link density, which is 1 at the gel point.

Using these equations, α, the fraction of structural units participating in cross-links, can be calculated from any set of G', $\overline{M}_n$, r and c. To compare theory and experiment, we start with a set of data $G'(t)$ corresponding to a known concentration of gelatin. Choosing $\overline{M}_n$ and r allows us to calculate α for each G'. The criterion for the goodness of fit is the comparison between the experimental gel time, approximated[8] by the time at which $G' = G''$, and the time at which $\alpha/\alpha_c = 1$. Two

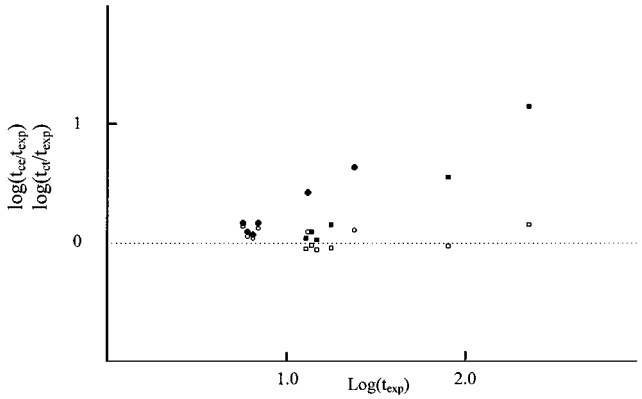

Figure 9. Comparison between experimental and calculated gel times for the six extracts at 3% and at 15 and 20 °C. Circles = 15 °C; squares = 20 °C; open symbols = using effective concentration (ce); solid symbols = using total concentration (ct).

average molecular weights and two cross-link functionalities were tested. Furthermore, the effect of the small molecular weight chains has been taken into account (polydispersity) to understand their influence on the elastic modulus according to the model.

In the first instance, the system is assumed to be monodisperse. The average molecular weight of the amino acid residue able to form a helix turn is taken as 500 in all the calculations. This allows the determination of the number of the structural units per chain as $\overline{M}_n/r$. The functionality of the cross-links was taken as either 4 (two chains involved) or 6 (three chains involved). The molecular weight-average used was either (i) the number-average weight obtained from the chromatogram with the concentration equal to the actual concentration, i.e., assuming that all the chains were involved in the network, or (ii) the molecular weight of an α chain (110 000) and the effective concentration (c_{eff}). Figure 9 shows a comparison of the calculated ($\alpha/\alpha_c = 1$) and experimental ($G''/G' = 1$) gel times for different combinations of functionality and average molecular weight of chains involved in the network's elasticity. The best agreement was obtained for a combination of a functionality of four, a molecular weight of the α chain and the effective, rather than the true, concentration. It is very satisfying to find that the best parameters for the network model are the same as those obtained by empirically fitting the experimental data.

We now briefly return to the fourth phase of the cure curve shown in Figure 2, which might be explained in the framework of the network model as due to the fusion of growing cross-links. This would decrease the number of junction zones (μ) at a constant number of EANCs (ν), leading to an increase in ξ and hence G (see eqs 3 and 5).

The effect of the polydispersity on the elasticity of the gel network has been tested using the model described above. Its effect is not straightforward. As well as changing G' through $\overline{M}_n$, the expressions for P and Q in eqs 6 and 7 also have to be changed; see ref 11 for details. The sample is assumed to be a mixture of 60% of α chains (M_w = 110 000) and 40% of smaller chains (M_w = 30 000). Figure 10 shows the calculated modulus as a function of α, the degree of reaction. The modulus of the polydisperse system is lower than when all the chains are assumed to be α chains. The calculations

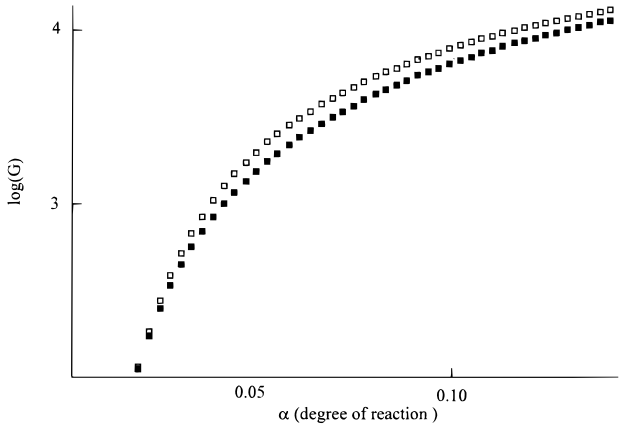

Figure 10. Effect of the polydispersity. Open squares: monodispersity of chain's molecular weight of 110 000. Solid squares: 60% of chain's molecular weight of 110 000 and 40% of chain's molecular weight of 30 000.

were repeated for several bimodal distributions. In all cases, introducing small chains decreased the elastic modulus. Conversely, it seems obvious that the introduction of large chains ("microgels") into the same calculation would increase the modulus. We conclude that this network model cannot explain the negligible gelling capacity of high molecular weight molecules.

A Kinetic Model for the Network Elasticity. Finally, given that both the master curve and network modeling imply that the elasticity is proportional to c^2, the gelation kinetics are compared to the predictions of a simple second-order reaction kinetics scheme. As explained above, the second-order reaction is visualized microscopically as being between an α chain which first loops back on itself and then reacts with a straight α chain to form a triple helix with four free ends

$$\mathrm{A} + \mathrm{B} \underset{k_2}{\overset{k_1}{\rightleftharpoons}} \mathrm{C}$$

with A representing the linear α chain, B the bent α chain, and C the resulting triple helix junction zone of functionality 4. k_1 is the rate constant for cross-link formation and k_2 that for cross-link melting.

The differential equation appropriate to this scheme is

$$\frac{\mathrm{d}x}{\mathrm{d}t} = k_1(a_0 - x)(b_0 - x) - k_2 x \tag{9}$$

where a_0 and b_0 are respectively the reactive site concentrations of A and B ($a_0 + b_0 = Nr$) and x is the cross-link concentration. In this scheme, a_0 and b_0 must be in the ratio 2:1. Other reactions, such as the condensation of three chains in configuration A would require other ratios. Equation 9 can be rewritten in the form

$$\frac{\mathrm{d}x}{\mathrm{d}t} = k_1(x - p)(x - q) \tag{10}$$

with

$$p = \frac{k_1(a_0 + b_0) + k_2 + \sqrt{{k_1}^2(a_0 - b_0) + 2k_1k_2(a_0 + b_0) + {k_2}^2}}{2k_1} \tag{11}$$

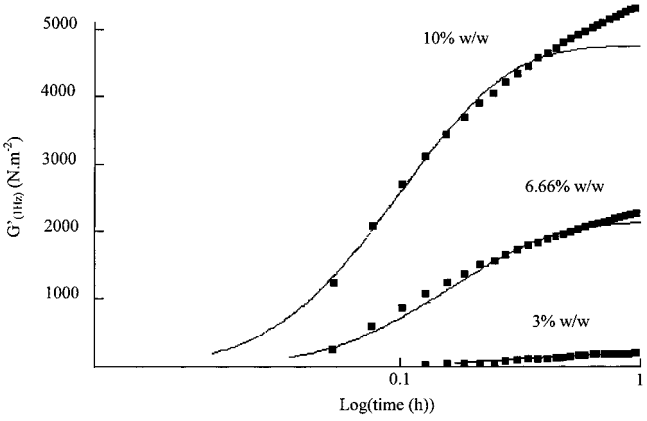

Figure 11. Comparison of experimental gelation kinetics at three concentrations with a calculation using the second-order reaction scheme and a single set of parameters. Sample E6, T = 10 °C.

and

$$q = \frac{k_1(a_0 + b_0) + k_2 - \sqrt{{k_1}^2(a_0 - b_0) + 2k_1k_2(a_0 + b_0) + k_2^2}}{2k_1} \tag{12}$$

The solution to eq 10 is

$$x = p\frac{1 - e^{k_1(p-q)t}}{1 - \frac{p}{q}e^{k_1(p-q)t}} \tag{13}$$

The cross-link concentration, x, can also be written αNr, where α is the degree of reaction for a given time. More generally, the evolution of the concentration of cross-links can be expressed as $x(t) = \alpha(t)\mathrm{Nr}$. Substituting into eq 13 gives

$$\alpha(t) = \left(\frac{p}{Nr}\right)\frac{1 - e^{k_1(p-q)t}}{1 - \frac{p}{q}e^{k_1(p-q)t}} \tag{14}$$

In the previous section it was shown that the degree of reaction $\alpha(t)$ can be related to the quantity ξ/N, which represents the network state. Thus, G' can be written as a function of the degree of reaction and so as a function of k_1, k_2, r, and time. Moreover, if the molecular weight of an α chain is known, and r, the number of reactive sites per chain is defined, the reaction extent can be written as a function of the molecular weight separating two reactive sites of the chain (M_0). Then

$$G(t) = \alpha(k_1,k_2,t,M_0)\frac{RTC}{M_\mathrm{n}} \approx G'(1\mathrm{Hz})(t) \tag{15}$$

Figure 11 shows the best fits obtained using this result for sample E6 at 10 °C and three different concentrations. The model fits the beginning of network formation well, but once the third phase, that we attribute to the growth of the cross-links begins, the model underestimates the elastic modulus. Clearly, a more sophisticated model is required to describe this third phase of the cure curve.

The parameters of the kinetic fit as a function of temperature, extract and concentration are shown in Tables 2−4, respectively.

Table 2. Effect of Cure Temperature on the Kinetic Constants for Sample E1, $c = 3\%$

temp (°C)	k_1 (mol^{-1} L min^{-1})	k_2 (min^{-1})	k_1/k_2 (mol^{-1} L)	M_0	t_{gel} (min) calcd	t_{gel} (min) measd
5	3×10^{-2}	1.3×10^{-3}	23	1200	2.5	<3.0
10	3×10^{-2}	1.3×10^{-3}	23	1300	3.0	<3.0
15	2×10^{-2}	1.0×10^{-3}	20	1400	6.0	6.1
20	0.9×10^{-2}	0.61×10^{-3}	15	1375	13.0	14.5

Table 3. Effect of Molecular Weight Distribution on the Kinetic Constants at 10%, $T = 15$ °C

extract	k_1 (mol^{-1} L min^{-1})	k_2 (min^{-1})	k_1/k_2 (mol^{-1} l)	M_0	t_{gel} (min) calcd	t_{gel} (min) measd
1	2×10^{-2}	1.0×10^{-3}	20	1350	1.5	<3.0
5	0.9×10^{-2}	1.8×10^{-3}	5	975	2.5	<3.0
6	0.45×10^{-2}	1.5×10^{-3}	3	810	4.0	4.5

Table 4. Effect of the Concentration on the Kinetic Constants for Sample E6 at 10 °C

concn (M)	k_1 (mol^{-1} L min^{-1})	k_2 (min^{-1})	k_1/k_2 (mol^{-1} L)	M_0	t_{gel} (min) calcd	t_{gel} (min) measd
3	0.5×10^{-2}	1.0×10^{-3}	5	800	15.0	14.0
6.66	0.6×10^{-2}	1.2×10^{-3}	5	800	4.0	<3.0
10	0.75×10^{-2}	1.5×10^{-3}	5	850	2.5	<3.0

The gel times calculated by the fit and reported in Table 2 are in good agreement with the experimental values. This indicates that the model is suitable for the early stages of gelation. The kinetic constant ratios do not change significantly with an increase in gelatin concentration (Table 4), which is expected. The molecular mass of the chain portion between two elastic centers varies according to three criteria:

•When the gelatin concentration increases, M_0 decreases (the number of junction zones per chain increases).

•When the temperature increases, M_0 increases (the number of junction zones per chain decreases).

•When the number of the extract increases, M_0 decreases, which is in good agreement with the effect of concentration.

Conclusions

The gelation kinetics of gelatin can be described as a succession of four different events. The present study has focused on the second and the third parts during which cross-links are formed and grow. Six different extracts of the same collagen with known molecular weight distributions have been investigated. Moreover, the effects of temperature, concentration, and effective concentration have been considered, and all the elasticity cure curves have been plotted on a master curve, by shifting horizontally and vertically the experimental data. From a practical point of view, the master curve can be used to predict the gelation kinetics of a gelatin sample over a wide range of conditions on the basis of very little data. Taken at face value, the model for the shift values can be used to extrapolate from the gel strength at a single time, temperature and concentration to predict the modulus at any other time, temperature and concentration within the ranges studied here. The dependence of elastic modulus on molecular weight distribution for gelatin is unique. We find by heuristics that the effect of the molecular weight distribution can be completely explained, to within experimental error, by supposing that only α, β, and γ chains contribute to the elasticity. Neither the small nor (more surprisingly) the high molecular weight fractions make any contribution. Note that we do not claim any absolute validity for these conclusions; we only assert that they explain our data completely. Nevertheless, for our six samples, which cover almost the whole range of commercially available gelling power, this model is a very good approximation for practical purposes. Given the molecular weight distribution of a gelatin sample an effective concentration can be calculated, which can then be used to make extrapolations.

The Pearson and Graessley model has been applied to gelatin gelation with some success. Using both experimental data and the restrictions of the model, the distribution of molecular weight can be simplified into two separate families of chains: those which are involved in the elasticity of the network (α, β, and γ chains) and others, which slow the progression of the network. The effective concentration of the gelatin to be taken into account when modeling the elasticity is the concentration of the fractions $\alpha + \beta + \gamma$.

A second-order model was used to fit the early stages of gelation, and the parameters of this reaction were interpreted at a molecular level. A more sophisticated kinetic model of the aging of the gelatin gels should improve the quality of our results. Moreover, the influence of the polydispersity, at least taking into account the small units and the α, β, and γ chains and the increase in the length of cross-links, should also improve our understanding of the gelation process.

It would be extremely interesting to extend the present study to lower concentrations and the early stages of gelation using light scattering, as Meunier et al.[10] have done for κ-carrageenan. They found that the shift factors for rheology and light scattering superposed, so that changes in structure correlate directly with changes in rheology, with no sign of any critical gelation concentration.

Having found that master curves exist for the gelation kinetics of two biopolymers with gels as different as those of gelatin and κ-carrageenan, it will be interesting to find whether other gelling biopolymers show the same behavior. Such master curves distill large amounts of experimental data, which is extremely useful for both theoretical studies and industrial practice.

Acknowledgment. This work was initiated during a sabbatical year that J.-C.R. spent at Elf-Atochem's research center in Lacq, France. It was then pursued by V.N. thanks to a thesis grant provided by Elf-Acquitaine. Tragically, a stroke prevented J.-C.R. from contributing to the writing of this paper.

References and Notes

(1) Veis, A. In *The macromolecular chemistry of gelatin;* Academic Press: New York and London, 1964.
(2) Te Nijenhuis, K. *Colloid Polym. Sci.* **1981**, *259*, 522−535.
(3) Clark, A. H. In *Food Polymers, Gels and Colloids*; Dickinson, E., Ed.; 1991; pp 322−338.
(4) Ross-Murphy, S. B. *Imaging Sci. J.* **1997**, *45*, 205−209.
(5) Coopes, I. H. *J. Polym. Sci.* **1970**, *A-1*, *8*, 1793.
(6) Benguigui, L.; Busnel, J. P.; Durand, D. *Polymer* **1991**, *32*, 2680−2685.
(7) Ferry, J. D.; Eldridge, J. E. *J. Phys. Chem.* **1949**, *53*, 184.
(8) Saunders, P. R.; Ward, A. G. In *Recent Advances in Gelatin and Glue Research*; Stainby, G., Ed.; Pergamon Press: Oxford, England, 1958; p 197.
(9) Saunders, P. R.; Ward, A. G. *Proc. 2nd Int. Congr. Rheol., Oxford* **1953**, 284.
(10) Meunier, V.; Nicolai, T.; Durand, D.; Parker, A. *Macromolecules* **1999**, *32*, 2610−2616.

(11) Pearson, D. S.; Graessley, W. W. *Macromolecules* **1978**, *11*, 528−533.
(12) Flory, P. J. *Proc. R. Soc. London, Ser A* **1976**, *351*, 351.
(13) Normand, V.; Ravey, J. C. *Rheol. Acta* **1997**, *36*, 610−617.
(14) Winter, H. H.; Chambon, F. *J. Rheol.* **1986**, *30*, 367−382.
(15) Mours, M.; Winter, H. H. *Rheol. Acta* **1994**, *33*, 385−397.
(16) Michon, C.; Cuvelier, G.; Launay, B. *Rheol. Acta* **1993**, *32*, 94−103.
(17) Llorente, M. A.; Mark, J. E. *J. Chem. Phys.* **1979**, *71*, 682−689.
(18) Higgs, P. G.; Ball R. C. *Macromolecules* **1989**, *22*, 2432−2437.
(19) Djabourov, M.; Leblond, J. *Am Chem Soc Symp. Ser.* **1987**, *350*, 211−223.
(20) Te Nijenhuis, K. *Colloid Polym. Sci* **1981**, *259*, 1017−1026.
(21) Te Nijenhuis, K. *Adv. Polym. Sci.* **1997**, *130*, 1.
(22) Oakenfull, D. G.; Scott, A. In *Gums and Stabilisers for the Food Industry*, 4th ed.; Phillips, G. O., Wedlock D. J., Williams, P. A., Eds.; IRL Press: Oxford, England, 1988; pp 127−134.
(23) Ross-Murphy, S. B. In *Food Polymers, Gels and Colloids*; Dickinson, E., Ed.; 1991; pp 357−368.
(24) Flory, P. J. *J. Am. Chem. Soc.* **1941**, *63*, 3083−3096.
(25) Scanlan, J. *J. Polym. Sci.* **1960**, *43*, 501.
(26) Case, L. C. *J. Polym. Sci.* **1960**, *45*, 397.
(27) Djabourov, M.; Papon, P. *Polymer* **1983**, *24*, 537−542.
(28) Durand, D.; Emery, J. R.; Chatellier, J. Y. *Int. J. Biol. Macromol.* **1985**, *7*, 315−319.

MA9909455